Direct Observation of Regulated Ribonucleoprotein Transport Across the Nurse Cell/Oocyte Boundary□ Ⅴ

Sarah Mische, Mingang Li, Madeline Serr, and Thomas S. Hays

Department of Genetics, Cell Biology, and Development, University of Minnesota, Minneapolis, MN 55455

In *Drosophila*, the asymmetric localization of specific mRNAs to discrete regions within the developing oocyte determines the embryonic axes. The microtubule motors dynein and kinesin are required for the proper localization of the determinant ribonucleoprotein (RNP) complexes, but the mechanisms that account for RNP transport to and within the oocyte are not well understood. In this work, we focus on the transport of RNA complexes containing *bicoid* (*bcd*), an anterior determinant. We show in live egg chambers that, within the nurse cell compartment, dynein actively transports green fluorescent protein-tagged Exuperantia, a cofactor required for *bcd* RNP localization. Surprisingly, the loss of kinesin I activity elevates RNP motility in nurse cells, whereas disruption of dynein activity inhibits RNP transport. Once RNPs are transferred through the ring canal to the oocyte, they no longer display rapid, linear movements, but they are distributed by cytoplasmic streaming and gradually disassemble. By contrast, *bcd* mRNA injected into oocytes assembles de novo into RNP particles that exhibit rapid, dynein-dependent transport. We speculate that after delivery to the oocyte, RNP complexes may disassemble and be remodeled with appropriate accessory factors to ensure proper localization.

INTRODUCTION

mRNA localization is used by a wide range of cell types as a means to restrict protein synthesis and activity. The resultant gradients or local elevations in protein concentration can direct the development of cell fates as well as modulate cellular functions (Lipshitz and Smibert, 2000; Kloc and Etkin, 2005; Shav-Tal and Singer, 2005). In *Drosophila*, the maternal mRNAs and proteins required for oocyte specification and growth are synthesized in nurse cells and delivered to the oocyte through the connecting ring canals (St Johnston, 2005; Steinhauer and Kalderon, 2006). Within the oocyte, the positional determinants that establish the major body axes of the embryo are deposited at discrete locations. For example, at the anterior pole, localized *bcd* mRNA is translated upon fertilization and directs formation of the anterior head and thoracic segments of the embryo. At the posterior pole, localized *oskar* mRNA triggers pole plasm assembly and specifies abdominal and germline development.

Recent studies suggest that both dynein and kinesin I motor proteins are required for the proper localization of maternal determinants (Brendza *et al.*, 2000; Duncan and Warrior, 2002; Januschke *et al.*, 2002; Palacios and St Johnston, 2002). However, it remains unclear which RNPs are actively transported along microtubules and by what motors. Motor proteins serve multiple functions in cells;

thus, disruption of motor function in oocytes could indirectly affect the localization of determinants. In addition, motor proteins may act cooperatively in the localization of RNPs (Brendza *et al.*, 2002; Duncan and Warrior, 2002; Januschke *et al.*, 2002). In this case, disruption of one motor's function could interfere with the activity of another motor, further complicating the interpretation of the outcome.

For transport events in the nurse cell compartment, previous studies suggest a model in which motors and associated cargoes move along a polarized microtubule track that leads from the nurse cells, through ring canals into the oocyte (Koch and Spitzer, 1983; Pokrywka and Stephenson, 1991; Theurkauf *et al.*, 1993). At mid-oogenesis (stages 7–9), the highly polarized microtubule cytoskeleton is reorganized. The cytoplasmic microtubules within the nurse cell compartment become randomly oriented, and a distinct cluster of microtubules assembles at the ring canals and extends into the nurse cell cytoplasm. The transport of maternal determinants along these microtubules was first directly visualized using a functional green fluorescent protein (GFP)-tagged Exuperantia (GFP-Exu) fusion protein. Exu assembles with *bcd* mRNA in nurse cells, and it is actively transported along microtubules to achieve proper localization of *bcd* mRNA at the anterior of the oocyte (Theurkauf and Hazelrigg, 1998; Cha *et al.*, 2001). Dynein is also known to accumulate in the early oocyte, and mutations in dynein block this accumulation (McGrail and Hays, 1997; Navarro *et al.*, 2004).

Within the oocyte, reorganization of the microtubule cytoskeleton is also a key event in the sorting of maternal mRNA determinants and embryonic patterning. Once delivered to the oocyte, anterior and posterior determinants are deposited at opposite ends, but the mechanisms underlying transport and localization are not well understood. Early models favored a polarized microtubule organization in which the minus end nucleation of microtubules was predominantly restricted to the anterior cortex and microtubule plus ends projected toward the posterior pole of the oocyte.

Table 1. Transport of GFP-Exu and GFP-Staufen in nurse cells

Genetic background	Velocity (μm/s $\pm$ SD)	p	Run-length (μm $\pm$ SD)	p	Particle n/sequence ($\pm$SD)	p	n particle (n sequence)
GFP-Exu							
Wild type	0.70 $\pm$ 0.19		5.08 $\pm$ 2.0		11 $\pm$ 3.8		101 (9)
UASp-ΔGl	0.53 $\pm$ 0.14	<0.0001	5.09 $\pm$ 2.2	0.9796	2.2 $\pm$ 1.9	<0.0001	31 (14)
Dhc-	0.39 $\pm$ 0.15	<0.0001	3.62 $\pm$ 1.6	0.0003	2.8 $\pm$ 1.4	<0.0001	25 (9)
Khc-	0.89 $\pm$ 0.25	<0.0001	5.73 $\pm$ 2.7	0.0202	13.9 $\pm$ 3.5	<0.0001	97 (7)
Klc-	0.87 $\pm$ 0.25	<0.0001	7.78 $\pm$ 2.3	<0.0001	12.5 $\pm$ 2.3	0.0028	75 (6)
Dhc- Rescue	0.70 $\pm$ 0.13	1.000	4.94 $\pm$ 1.9	0.5962	10.4 $\pm$ 4.9	0.3537	83 (8)
Khc- Rescue	0.72 $\pm$ 0.16	0.3663	4.97 $\pm$ 1.8	0.6444	11.1 $\pm$ 1.9	0.8143	100 (9)
GFP-Staufen							
Wild type	0.84 $\pm$ 0.26		5.35 $\pm$ 2.7		12 $\pm$ 3.5		108 (9)
UASp-ΔGl	0.65 $\pm$ 0.24	0.0029	4.20 $\pm$ 1.8	0.0715	2.4 $\pm$ 2.2	<0.0001	17 (7)
Dhc-	0.61 $\pm$ 0.15	<0.0001	4.16 $\pm$ 1.5	<0.0001	9.6 $\pm$ 1.5	<0.0001	86 (9)
Khc-	1.05 $\pm$ 0.39	<0.0001	7.15 $\pm$ 3.7	<0.0001	13.7 $\pm$ 2.8	0.0088	96 (7)
Dhc- Rescue	0.80 $\pm$ 0.21	0.2272	5.78 $\pm$ 2.4	0.2198	12.2 $\pm$ 2.6	0.9279	73 (6)
Khc- Rescue	0.87 $\pm$ 0.20	0.3069	5.32 $\pm$ 1.9	0.9191	12.1 $\pm$ 1.7	0.6100	97 (8)

Average calculated velocities, run-lengths, and particle number for GFP-Exu and GFP-Staufen in a wild-type background were directly compared with those from each of the mutant backgrounds. Values represent mean $\pm$ SD. $p < 0.05$ is statistically significant. Dhc-, *Dhc6-6/Dhc6-12*; Khc-, *Khc[27]*; Klc-, *klc[8ex94]*.

Based on this polarity, plus end motors were predicted to deposit posterior determinants, whereas minus ends motors delivered determinants to the anterior cortex. However, more recent studies suggest there is no simple polarized array of microtubules that spans the anterior–posterior axis (Cha *et al.*, 2001). Instead, microtubules seem to nucleate along the entire cortex and project at random directions to generate a microtubule network. How determinants become targeted to the anterior and posterior poles of the oocyte remains to be explained. In late stages of oogenesis, maintenance of *bcd* at the anterior of the oocyte seems to require continual transport (Weil *et al.*, 2006). Whether dynein and kinesin actively transport RNP determinants along microtubules is only beginning to be addressed by the direct visualization of RNP transport in wild-type and mutant backgrounds (Weil *et al.*, 2006). In an alternative mechanism known as cytoplasmic streaming, RNPs may be moved nonspecifically throughout the ooplasm and then selectively retained by localized anchors at the proper locations (Glotzer *et al.*, 1997; Forrest and Gavis, 2003). Although it is known that microtubules and the kinesin motor are required for cytoplasmic streaming, the extent to which this process contributes to the localization of anterior and posterior determinants is uncertain.

In the present study, we directly test the role of dynein and kinesin I in the active transport of the *bcd* anterior determinant in live egg chambers. We use GFP-Exu as well as fluorescently labeled *bcd* RNA to monitor the motile behavior of *bcd* RNPs in nurse cells and mid-staged oocytes. The fast acquisition of images allows us to visualize and quantitate the directed transport of RNPs along microtubules in wild-type and motor mutant backgrounds. The results show that dynein actively transports the *bcd* determinant along microtubules within the nurse cells and oocyte.

MATERIALS AND METHODS

Fly Stocks

GFP-Exu was a gift from Tulle Hazelrigg (Columbia University). *GFP-Staufen* was a gift from Daniel St Johnston (University of Cambridge). *FRT42B Khc[27]/ CyO, yw hs-Flp; Sco/CyO* and *w; Sco/CyO; Pk15a* were gifts from Bill Saxton

(Indiana University). *klc[8ex94] FRT2A/TM3 Sb* was a gift from Isabel Palacios (University of Cambridge). *nanos-GAL4 VP16* was a gift from Ruth Lehman (New York University School of Medicine). The *FRT42B ovo[D1], elav-GAL4,* and *GFP-alphaTub84B* stocks were obtained from the Bloomington Stock Center (Bloomington, IN). Dynein heavy chain mutations *Dhc64C6-6* (hereafter called *Dhc6-6*) and *Dhc64C6-12* (*Dhc6-12*) are described in Gepner *et al.*, 1996. *Dhc64C* transgenic flies are described in McGrail and Hays, 1997. OregonR were wild-type flies, except where noted.

Genetic Crosses

Dhc64C mutant ovaries were generated from *w; Dhc6-12/TM6B* males crossed to *GFP-Exu; Dhc6-6/TM6B* or *GFP-Staufen, Dhc6-6/TM6B* virgins. Progeny expressing *GFP-Exu* or *GFP-Staufen* in the *Dhc6-6/Dhc6-12* background were examined; balanced siblings were used as controls. To analyze *UASp-ΔGl* expression in ovaries, *GFP-Exu* or *GFP-Staufen* virgins were crossed to *UASp-ΔGl/CyO; nos-GAL4/TM6B* males. Progeny expressing *UASp-ΔGl* and *nos-GAL4* in the *GFP-Exu* or *GFP-Staufen* background were examined; control siblings lacked the *nos-GAL4* driver. Neuronal expression of the *UASp-ΔGl* construct was driven with the *elav-GAL4* driver. All germline clones were generated by the FLP recombinase system (Chou *et al.*, 1993; Chou and Perrimon, 1996) using *ovo[D1]* (Granadino *et al.*, 1992). Eggs were collected for 2–3 d and then larvae were heat shocked as first, second, and third instar for 2 h at 37°C.

Confocal Imaging in Living Egg Chambers

Ovaries were dissected into halocarbon oil, and individual egg chambers were teased apart. Each sample was derived from a separate female [Table 1, *n* particle (*n* sequence)]. Images were acquired using a Nikon Eclipse TE200 inverted microscope equipped with the PerkinElmer confocal imaging system (PerkinElmer Life and Analytical Sciences, Boston, MA), and Hamamatsu's Orca-ER digital camera. GFP-particle movements in nurse cells were captured at 1-s intervals and 2 $\times$ 2 binning by using a 60$\times$ Planapo (numerical aperture [NA] 1.4) objective. Cytoplasmic streaming was imaged at 30-s intervals, with five optical Z-sections of 2-μm spacing using a 40$\times$ Planfluor (NA 1.3) objective. GFP-Exu particle disassembly was imaged at 1-s intervals, with 12, 2-μm optical sections and 2 $\times$ 2 binning using a 100$\times$ Planapo (NA 1.4) objective. GFP-particle localization (Supplemental Figure 3) was imaged with 1 $\times$ 1 binning and a 40$\times$ Planfluor objective, and optical sections of 1 μm were collected.

Immunohistochemistry

Ovaries used for fixed analysis had the same genotype as those described above for the motility analyses, although lacking the GFP-transgenes. Ovaries were dissected, fixed, and prepared as described previously (McGrail and Hays, 1997). Microtubules were visualized with a fluorescein isothiocyanate-conjugated DM1A anti-α-tubulin antibody (1:200; Sigma-Aldrich, St. Louis, MO). Actin was visualized using tetramethylrhodamine B isothiocyanate-labeled phalloidin (1:1000; Sigma-Aldrich). The distribution of cytoskeletal

filaments was imaged with a 40× Planfluor or 100× Planapo objective by using 1 × 1 binning with optical sections of 1 μm.

Rate Analysis

GFP-tagged RNP velocity and run-length were manually tracked with Meta-Morph (Molecular Devices, Sunnyvale, CA) image analysis software's "track points" function. Each particle displaying movement in a linear manner for four consecutive frames was selected for analysis. The cursor was placed at the leading edge of each particle in the direction of the movement. The X and Y positions of this particle were recorded. As the particle moved in each subsequent frame, the cursor was moved to the new position of the leading edge, and the new X and Y positions of this particle were recorded. This procedure continued until the particle ceased moving, or moved out of the plane of focus; consequently, the measurements of run-lengths are underestimates.

Intensity Measurements

Intensity measurements were performed with MetaMorph (Molecular Devices) image analysis software's "region measurements" function. Particle intensity measurements were derived from seven egg chambers. For each egg chamber, the average intensity of 12 particles within the nurse cells, and 12 particles within the oocyte were determined. A circle of 1.69 μm^2 in area was used for all the measurements. For measurements of cytoplasmic intensity, 17 egg chambers were examined. For each egg chamber, the average intensity of five 5-μm-long line-scans in the nurse cells and in the oocyte was determined. All line-scans were perpendicular and adjacent to the nurse cell/oocyte membrane, and they were placed where there were no formed particles present. Mean intensities were calculated for the nurse cells and the oocyte.

Statistical Calculations

The average velocity and total run-length for each motile particle were calculated using Excel (Microsoft, Redmond, WA), as was the SD for velocity and run-lengths for all particles measured in each genotype. The velocity, run-length, and frequency for each mutant genotype were directly compared with those of wild-type controls. All statistical significance calculations were determined by using the Student's t test on unpaired data with unequal variance. Significance was established if the resulting p value was <0.05.

Injection of Fluorescently Labeled bcd mRNA

Full-length *bcd* mRNA was prepared by in vitro transcription as described in Cha and Theurkauf (2001). *bcd* mRNA was injected into the oocytes of wild-type, *Khc^{27}* and *UASp-ΔGl* egg chambers, or, in some experiments, injected into nurse cells and then transferred to wild-type or mutant oocytes. To examine cortical localization, time-lapse sequences were acquired at 60× Planapo objective by using 2 × 2 binning collecting five optical sections at 2-μm intervals, at a time interval of 30 s for 10 min. *bcd* particle transport sequences in oocytes were acquired with a 100× Planapo objective using 2 × 2 binning with 1-s exposure for 2–3 min. Colocalization studies of GFP-Exu and *bcd* were acquired with a 100× Planapo objective by using 2 × 2 binning with 1-s exposure for each wavelength, and a settle frame.

RESULTS

Nurse Cell Transport of Exu RNP Complexes

To determine which motors are active in RNP transport within nurse cells, we first characterized the baseline properties (velocity, run-length, and frequency) of GFP-Exu particle transport in wild-type stage 8–9 egg chambers (Table 1). The GFP-tagged Exu gene product assembles into *bcd* RNPs in vivo and moves in a linear, microtubule-dependent manner (Figure 1, Supplemental Figure 1, and Movie S1). Treatment of the egg chambers with colcemid eliminates all particle movements in nurse cells (Figure 1B). In wild-type egg chambers, the average velocity of GFP-Exu transport in nurse cells was 0.70 ± 0.19 (SD) μm/s. Typically, we observe runs showing continuous velocity over an average distance of 5.08 ± 2.0 μm (Table 1). Our data extends previous studies of the GFP-Exu complex (Wilhelm *et al.*, 2000; Cha *et al.*, 2001).

At the face of the ring canals leading to the oocyte, we observe an array of microtubules extending 5–10 μm into the nurse cell cytoplasm (Figure 2; also see Theurkauf and Hazelrigg, 1998). The elevated microtubule concentration at the ring canal may facilitate RNP movements toward and through the ring canal. At greater distances from the ring
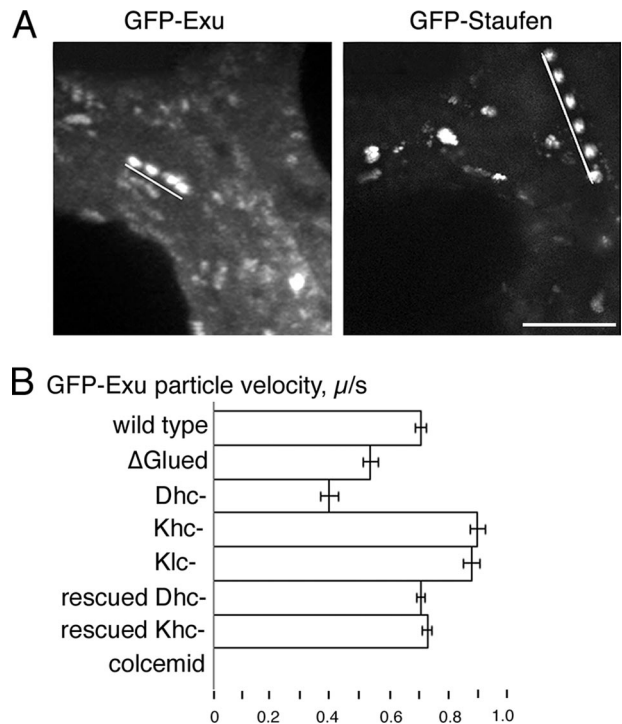

Figure 1. Quantification of GFP-RNP motility in nurse cells. (A) Time-lapse projections highlight linear movements of GFP-Exu (4 s) and GFP-Staufen (6 s) (Supplemental Movies S1 and S2). White lines indicate the path of a single particle within nurse cells. Bar, 5 μm. (B) Comparison of average velocities of GFP-Exu transport events in the nurse cells of wild-type, mutant, and colcemid-treated egg chambers. Disruption of dynein and kinesin I have opposite effects on the calculated velocities. Effects of the dynein and kinesin I mutations are fully rescued by their respective wild-type transgenes. On treatment with colcemid, GFP-Exu RNPs failed to undergo transport. Similar results were obtained for GFP-Staufen (Table 1). Dhc-, *Dhc6-6/Dhc6-12*; Khc-, *Khc^{27}*; Klc-, *klc^{8ex94}*. Error bars indicate SE of the mean.
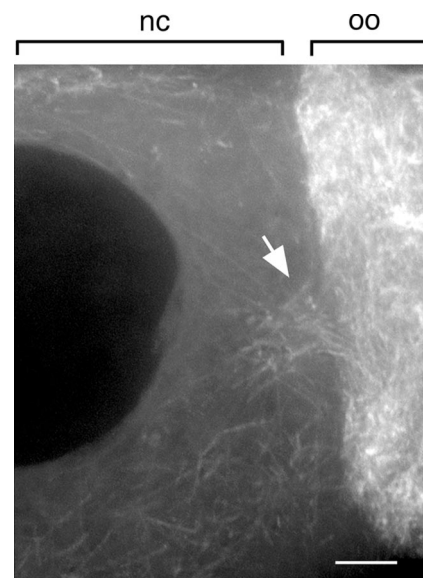

Figure 2. Microtubule distribution at the ring canals leading into the oocyte. Within the nurse cells (nc), microtubules seem to be oriented randomly; however, near the ring canals (arrow), the number and organization of microtubules increases. Shown is a projection of eight 0.5-μm optical sections. oo, oocyte, Bar, 5 μm.

canal, particles are less likely to encounter the ring canal microtubule array, and their movements are along the more randomly oriented microtubules that are present throughout the nurse cell cytoplasm (also see Theurkauf and Hazelrigg, 1998).

Dynein Is Required for Transport of Exu in Nurse Cells

To test whether dynein actively transports GFP-Exu in nurse cells, we disrupted dynein function by two independent strategies and scored the resulting defects in RNP transport. First, we disrupted dynactin function. The dynactin complex associates with dynein, and we showed previously that expression of a truncated p150-Glued subunit acts as a dominant negative inhibitor of dynein function (McGrail *et al.*, 1995). For the present study, we built and verified a transgene, *UASp-ΔGl*, based on the original *Glued¹* dominant mutation (Swaroop *et al.*, 1987) and controlled via the UAS-GAL4 system (Brand and Perrimon, 1993; Rorth, 1998) (Supplemental Figure 2, Supplemental Materials and Methods).

The transport of GFP-Exu particles in nurse cells is dramatically reduced by moderate expression of the dominant-negative Glued construct UASp-ΔGl (Table 1). When expression of a single *UASp-ΔGl* transgene is driven by one copy of the germline-specific *nanos-GAL4* driver, the number of motile GFP-Exu particles per sequence was reduced fivefold (11 ± 4.2 in wild-type compared with 2.2 ± 1.9; $p < 0.0001$). The small number of GFP-Exu particles that still moved exhibited an average velocity of $0.53 \ \mu m/s \pm 0.14$ ($p < 0.0001$), significantly slower than the velocity observed in the wild-type background (Table 1).

Our second method of disrupting dynein function to determine its impact on RNP particle transport uses mutations in the dynein heavy chain. A transheteroallelic combination of the dynein heavy chain alleles, *Dhc6-6* and *Dhc6-12*, is known to reduce the level of dynein activity. The oocyte is specified and development proceeds through late oogenesis but ultimately results in female sterility (Gepner *et al.*, 1996). In this dynein mutant background, all aspects of GFP-Exu particle motility are significantly affected (Table 1). The number of transport events drops to an average of fewer than three motile particles per recorded sequence. The average velocity of GFP-Exu particles is also reduced ($0.39 \pm 0.15 \ \mu m/s$; $p < 0.0001$), and the run-length decreased to $3.62 \pm 1.6 \ \mu m$ ($p = 0.0003$). The defects in GFP-Exu RNP motility are specifically due to the loss of dynein activity, because a wild-type *Dhc64C* transgene fully restores wild-type transport properties in the *Dhc6-6/Dhc6-12* mutant egg chambers (Table 1).

Is the requirement for dynein-based transport in nurse cells specific for anterior determinants? To address this question, we asked whether transport of the posterior determinant Staufen also depends on dynein function. In wild-type egg chambers, GFP-Staufen complexes move along linear tracks of microtubules at an average rate of $0.84 \pm 0.26 \ \mu m/s$ with an average run-length of $5.35 \pm 2.7 \ \mu m$ (Supplemental Movie S2). The distribution of the wild-type GFP-Staufen velocities falls into a single peak that is distinct from that observed for the GFP-Exu velocities, suggesting that they form distinct RNP particles. Our analysis shows that the UASp-ΔGl and *Dhc6-6/Dhc6-12* mutant backgrounds also significantly disrupt transport of GFP-Staufen particles (Table 1).

A Kinesin Null Mutation Accelerates Transport in Nurse Cells

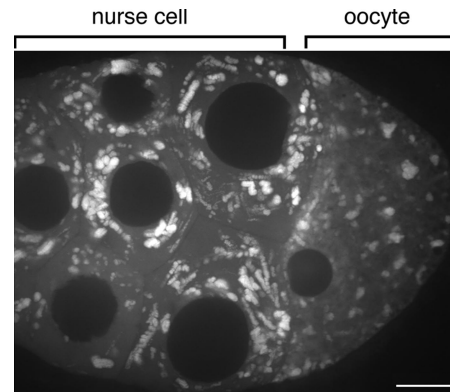We extended our in vivo analysis to ask whether kinesin I also contributes to the transport of the GFP-Exu particles

nurse cell   oocyte

Figure 3. The compartmentalization of rapid cytoplasmic movements is illustrated by this 3-min time-lapse projection of GFP-Exu particles. Within the nurse cells, the RNPs exhibit robust linear transport. By contrast, in the oocyte, linear cytoplasmic movements of RNPs are not detectable over this timeframe (Supplemental Movie S3). The same phenomenon was observed for GFP-Staufen. Bar, 20 μm.

within nurse cells. To eliminate kinesin I function, we generated germline clones that were homozygous for the kinesin heavy chain null allele *Khc²⁷* (Brendza *et al.*, 2000). Unexpectedly, we found that kinesin I seems to act as an antagonist of dynein-mediated transport of GFP-Exu within the nurse cell compartment. The velocities, run-lengths, and frequencies of transport were significantly elevated for both GFP-Exu and GFP-Staufen (Table 1). Expression of a wild-type *Khc* transgene in the *Khc* null egg chambers restores the normal transport properties observed in wild-type nurse cells (Table 1) and demonstrates that the elevated transport results specifically from the loss of kinesin I function. Elevated velocities of RNP transport are also observed in germline clones mutant for the kinesin light chain, which suggests that kinesin I binds RNPs through the light chain subunit (Table 1). Our data indicate that kinesin I negatively regulates dynein transport in the nurse cell compartment.

GFP-Exu Transport Is Regulated at the Nurse Cell/Oocyte Boundary

The transport of GFP-Exu in the nurse cell compartment is rapid and occurs along linear tracks. In contrast, the movement of GFP-Exu particles is significantly slower once they pass through the ring canals leading into the oocyte (Figure 3 and Supplemental Movie S3). The linear tracks of particle motility characteristic within nurse cells are absent in the oocyte. This result indicates that motor-dependent movement of GFP-Exu particles is down-regulated as the particles cross the ring canal entering the oocyte.

The GFP-Exu and -Staufen particles that move into the oocyte are not entirely static, but they exhibit slower movements consistent with cytoplasmic streaming (Theurkauf, 1994; Glotzer *et al.*, 1997; Palacios and St Johnston, 2002). This slower movement within the oocyte is readily detected when the rate of image acquisition is decreased (Figure 4). In mid-oogenesis, cytoplasmic streaming is slow and uncoordinated (Palacios and St Johnston, 2002). In later stage 10b oocytes, the rate and organization of streaming increase markedly, and the bulk of the cytoplasm moves unidirectionally and orthogonal to the long axis of the oocyte.

Whether the dynein motor helps to power cytoplasmic streaming is not clear. To test this possibility, we scored cytoplasmic streaming rates in both mid- and late-stage
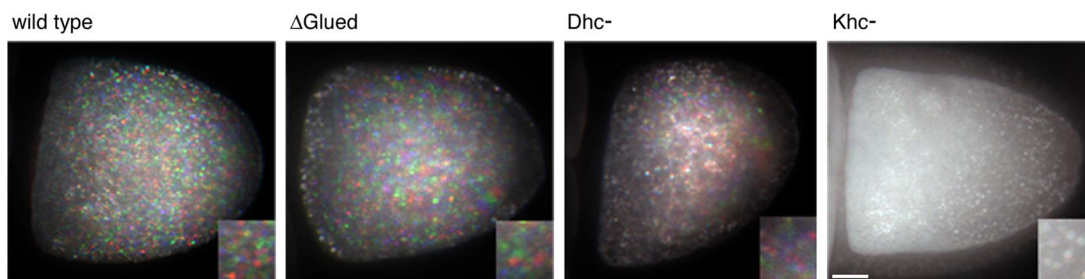
Figure 4. Cytoplasmic streaming does not require dynein. Three sequential images of autofluorescent yolk particles in stage 10b egg chambers were pseudocolored red, green, or blue with MetaMorph software and then superimposed. The resulting images reveal the presence or absence of movement as determined by the presence or absence of color. Moving particles display the red, green, blue color sequence, whereas the superimposition of images of nonmotile particles occurs as a single white particle. ΔGl and *Dhc6-6/Dhc6-12* oocytes show a color pattern similar to wild-type, but *Khc27* egg chambers show no movement in the oocyte (Supplemental Movie S4). Bar, 20 μm. Insets show 2.5× magnification.

oocytes expressing UASp-ΔGl. Despite the strong inhibition of dynein function by UASp-ΔGl expression, cytoplasmic streaming in the oocyte is not affected (wild-type: 0.22 ± 0.11 μm/s; ΔGl: 0.21 ± 0.07 μm/s; Figure 4 and Supplemental Movie S4). Similarly, we find no change in cytoplasmic streaming in oocytes from the dynein mutant background, *Dhc6-6/Dhc6-12* (Figure 4). However, cytoplasmic streaming is completely arrested in *Khc27* egg chambers (Figure 4), consistent with previous reports (Palacios and St Johnston, 2002; Serbus *et al.*, 2005). By comparison, streaming is not arrested, but only slightly reduced in *klc8ex94* mutant clones (also see Palacios and St Johnston, 2002).

The size and shape of the *bcd* RNP particles change upon entering the oocyte. We followed the fragmentation and/or complete disassembly of Exu RNP particles as they entered the oocyte from the nurse cell compartment (Figure 5 and Supplemental Movie S5). RNP particles observed in the oocyte exhibit a 19% lower fluorescence intensity than those particles in nurse cells ($p < 0.0001$), and the surrounding ooplasm shows a 25% elevation in the level of fluorescence compared with nurse cell cytoplasm ($p < 0.0001$).

Exu Localization Within the Oocyte Depends on Dynein Function

Although the active transport of RNPs entering the oocyte is suppressed relative to nurse cell transport, our data show that dynein is nonetheless required for anterior accumulation of GFP-Exu (Supplemental Figure 3A). In wild-type, mid-stage oocytes, GFP-Exu accumulates to the anterior (Wang and Hazelrigg, 1994); conversely, GFP-Staufen accumulates to the posterior cortex (Palacios and St Johnston, 2002). Disruption of dynein function by UASp-ΔGl or *Dhc6-6/Dhc6-12* eliminates the anterior localization of GFP-Exu, whereas the posterior accumulation of GFP-Staufen is unaffected (Supplemental Figure 3A). Moreover, the introduction of a wild-type *Dhc64C* transgene is sufficient to rescue GFP-Exu localization (data not shown).

GFP-Exu has also been observed to accumulate along the posterior cortex in late stage 9 and 10a oocytes (Lin *et al.*, 2006). We find that when the anterior accumulation of GFP-Exu is blocked by inhibiting dynein function, the subsequent posterior accumulation of GFP-Exu is also blocked (n = 12; Supplemental Figure 3B). This result suggests that late posterior localization of Exu is dependent on the earlier anterior localization, but the basis for this dependency is unclear.

The kinesin I-dependent process of cytoplasmic streaming may facilitate the random delivery of RNPs to the cortex for localization. If so, then the arrest of cytoplasmic streaming would be expected to diminish anterior as well as posterior accumulation. The localization of GFP-Exu at the anterior of the oocyte is largely retained in the *Khc* null egg chambers, although somewhat less tightly focused (Supplemental Figure 3A). In contrast, GFP-Staufen accumulation to the posterior is completely lost. Together, our results demonstrate
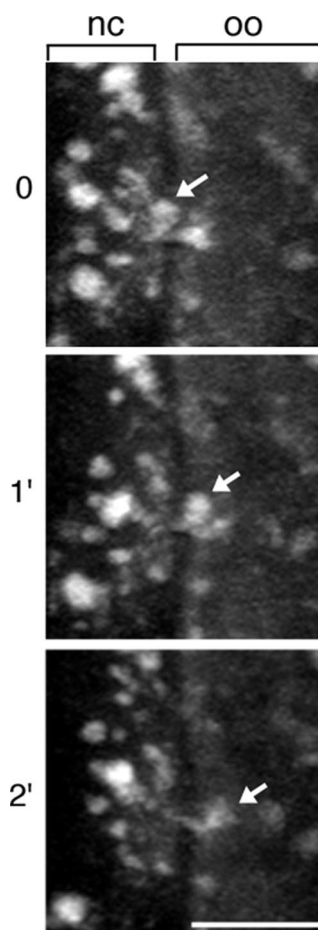

Figure 5. RNP disassembly. After transport into the oocyte, GFP-Exu particles seem to decrease in size and/or disappear. Optical sections spanned sufficient depth to ascertain that the particle did not simply leave the focal plane. Arrow highlights a single particle undergoing this process as it enters the oocyte (Supplemental Movie S5). Bar, 10 μm, nc, nurse cell; oo, oocyte.

that the dynein requirement for Exu localization is independent of kinesin.

Transport of *bcd* mRNA in the Oocyte Depends on Dynein Function, but Not Kinesin I Function

To test the hypothesis that dynein transports *bcd* mRNA in the oocyte, we imaged the behavior of fluorescently labeled *bcd* mRNA injected into wild-type and mutant egg chambers. After direct injection into wild-type oocytes *bcd* mRNA accumulates at the anterior and/or lateral cortices of the oocyte (Figure 6A wild-type panel and Supplemental Movie S6; also see Cha *et al.*, 2001). We find that GFP-Exu is recruited to the injected RNA in the oocyte (Supplemental Figure 1B), as was previously reported for the injection of *bcd* RNA into nurse cells (Cha *et al.*, 2001). This suggests that Exu retains an association with at least some population of *bcd* RNPs within the oocyte. To test whether dynein is the motor involved in the transport and cortical accumulation, we injected the *bcd* mRNA into oocytes expressing UASp-ΔGl. The *bcd* mRNA slowly diffused from the site of injection, but it failed to accumulate to the cortex in the UASp-ΔGl egg chambers (Figure 6A UASp-ΔGl panel and Supplemental Movie S7). In contrast, elimination of kinesin I activity in *Khc*[27] oocytes did not affect the transport or cortical accumulation of the injected *bcd* mRNA (Figure 6A, *Khc*[27], and Supplemental Movie S8).

bcd RNA injected into nurse cells may recruit additional nurse cell factors that act to restrict *bcd* accumulation to the anterior cortex (Cha *et al.*, 2001). We examined whether such factors might influence the transport of *bcd* RNP within the oocyte. Following the approach of Cha *et al.* (2001), we injected *bcd* RNA into nurse cells, withdrew the assembled RNPs, and reinjected them into the oocyte. As reported previously, we find that the transferred *bcd* RNPs frequently accumulate at the anterior cortex (9 of 11 injections). We did, however, observe accumulation at both lateral and anterior cortices in a subset of the oocytes (2 of 11 injections). In all samples examined, cortical accumulation was dependent on dynein (n = 11), and not kinesin (n = 10), just as we observed for *bcd* RNA injected directly into oocytes.

At high magnification, we characterized the rapid transport of small RNP particles that assemble de novo following the injection of fluorescent *bcd* mRNA directly into oocytes (Figure 6B and Supplemental Movie S9; Table 2). The movement of *bcd* RNPs is microtubule-dependent and is blocked by the coinjection of colcemid (Cha *et al.*, 2001). Within the oocyte, microtubules are organized as a meshwork of fibers extending from the cortex and into the oocyte cytoplasm (Figure 6C). There is a higher concentration of microtubules at the anterior of the oocyte, relative to their concentration at the posterior. Consistent with the arrangement of microtubules, the de novo *bcd* RNPs are rapidly transported (0.55 ± 0.15 μm/s) in random directions, but with an apparent bias toward the anterior pole (Figure 6B and Table 2). We calculated similar velocities for *bcd* mRNA injected to *Khc* null oocytes confirming that kinesin I is not essential for the transport of *bcd* mRNA within the oocyte. In contrast, *bcd* mRNA injected into UASp-ΔGl mutant oocytes exhibits a significantly reduced transport rate and run length. The fluorescence signal from RNPs assembled in nurse cells and transferred into the oocyte is reduced by dilution and prevents an analysis of individual particle movements within the oocyte. Nonetheless, the transferred RNPs accumulate at the cortex in a dynein-dependent manner.
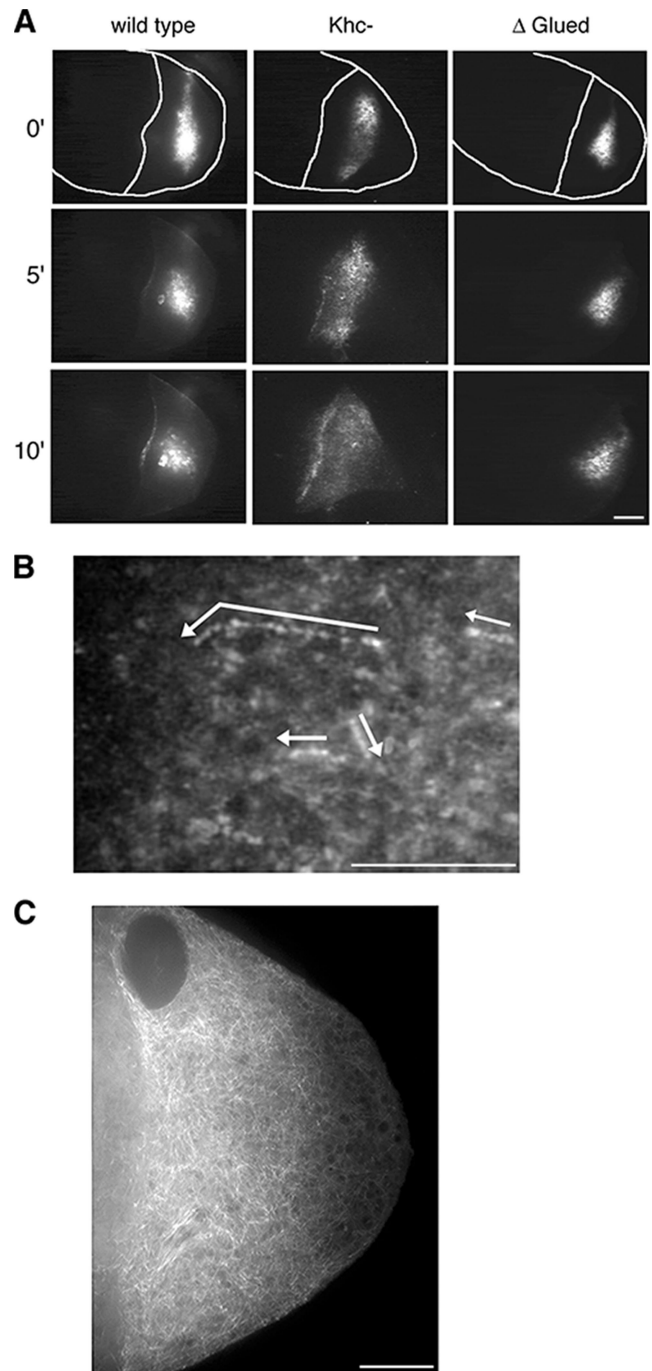

Figure 6. Fluorescently labeled *bcd* mRNA. (A) *bcd* RNA injected to the oocyte accumulates to the cortex in wild-type and *Khc*[27] egg chambers. In contrast, this cortical accumulation is blocked in the UASp-ΔGl background. Still images from acquired time-lapse sequences at 0, 5, and 10 min after injection of *bcd* (Supplemental Movies S6–S8). Tracings of the egg chamber highlight the oocyte cortex. Bar, 20 μm. Throughout this figure, anterior is to the left, and posterior is to the right. (B) A time-lapse projection of 26 images reveals the tracks of *bcd* mRNA particles moving in a linear manner. Arrows indicate their direction of transport. Particles corresponding to the arrows are enhanced for clarity in this still image. Supplemental Movie S9. Bar, 10 μm. (C) Microtubule distribution within the oocyte as revealed with UAS-α-tubulin-GFP. Note the meshwork appearance of the microtubule array. A higher concentration of microtubules is present at the anterior cortex, compared with the posterior cortex. Bar, 10 μm.

Table 2. Transport of injected *bcd* mRNA in the oocyte

Genetic background	Velocity (μm/s $\pm$ SD)	p	Run-length (μm $\pm$ SD)	p	*n* particle (*n* sequence)	Particle direction (anterior:posterior)
Wild type	0.55 $\pm$ 0.15		3.1 $\pm$ 1.2		52 (4)	32:20
Khc-	0.53 $\pm$ 0.15	0.5002	2.8 $\pm$ 1.1	0.1892	51 (4)	34:17
UASp-ΔGl	0.44 $\pm$ 0.10	<0.0001	2.2 $\pm$ 0.70	<0.0001	46 (14)	30:16

The calculated velocities for *bcd* particle transport in the oocytes of wild-type, *Khc* null, and UASp-ΔGl egg chambers. Dynein is required for the nonpolar transport of *bcd* within the oocyte.

The Actin Cytoskeleton Is Disrupted Within the Oocyte of Khc Null Egg Chambers

Both the microtubule and actin cytoskeletons contribute to the regulation of cytoplasmic streaming and RNP localization within the oocyte (Theurkauf, 1994; Emmons *et al.*, 1995; Rosales-Nieves *et al.*, 2006). Thus, any disruption of microtubule and/or actin filament organization by our mutant backgrounds could indirectly disrupt transport and localization of determinants described in our studies. To address this concern, we fixed ovaries from wild-type and microtubule motor mutant backgrounds, and we characterized the cytoskeletal organization of the egg chambers (Supplemental Figure 4). We find no significant difference in the microtubule network between wild-type and mutant egg chambers. Similarly, the actin distribution in wild-type and dynein mutant backgrounds are indistinguishable from each other. However, we did detect an aberrant actin cytoskeleton in the kinesin I mutant oocytes. The cortical actin network is less uniform, and we observe hollow spheres of actin within the cytoplasm of most oocytes (Supplemental Figure 4, inset). This unusual phenotype was previously described for strong alleles of *swallow* that fail to localize *bcd* mRNA to the anterior cortex (Meng and Stephenson, 2002). These results raise the possibility that strong loss-of-function kinesin I alleles affect cytoplasmic streaming and RNP localization by disturbing actin organization.

DISCUSSION

Our results demonstrate that dynein actively transports Exu and *bcd* mRNA, components required for the establishment of anterior polarity in oocytes. We show that partial loss of either dynein or dynactin function reduces both the velocity and frequency of GFP-Exu particle transport (Figure 1B and Table 1). The velocities of all the motile Exu RNP particles were reduced; there is no subpopulation of unaffected particles, suggesting that dynein is required for all particle transport. Additionally, our observations show that disruption of dynein inhibits polarized transport of GFP-Exu across the ring canal and blocks oocyte growth (Supplemental Movie S10), consistent with microtubule-dependent transport across the ring canals.

We identify dynein as the motor required for transport of both anterior and posterior determinants. GFP-Exu and -Staufen as well as additional RNP components (e.g., dImp; work to be reported elsewhere) depend on dynein for transport from nurse cells to the oocyte. Interestingly, the average velocity of GFP-Staufen particles is significantly faster than the transport of GFP-Exu (p < 0.0001). These observations suggest that although dynein-based transport from nurse cells to the oocyte is conserved among RNP complexes, the number of motors, their linkage, and/or their regulation may differ between mRNA complexes. Indeed, recent observations suggest that distinct mRNAs may differentially recruit motor proteins as well as potential regulators of motor activity (Bullock *et al.*, 2006).

Significantly, the loss of kinesin activity accelerates the velocity of the GFP-Exu RNPs. Previous studies of fixed ovaries have shown that kinesin I function is required within the oocyte for *oskar* localization, but they suggested that kinesin I is not involved in RNP transport within nurse cells (Brendza *et al.*, 2000; Palacios and St Johnston, 2002). Our analysis in living cells supports the conclusion that kinesin I is present on RNP particles in the nurse cells and that it functions to negatively regulate dynein-mediated RNP transport (Figure 1B and Table 1).

One possible explanation for this result is that RNP transport in nurse cells is bidirectional, with rapid switching between the dynein and kinesin motors. Although we do not observe bidirectional motion, brief reversals (<1 s) in direction are below our spatiotemporal resolution. Alternatively, the two types of motors may be engaged in a constant tug-of-war in which dynein activity overpowers kinesin and drags the particle unidirectionally. In either case, the elimination of kinesin would reduce the load on the dynein motors, yielding elevated rates of transport. A third possibility is that both kinesin and dynein bind to the same receptor on the Exu (or Staufen) RNP, but kinesin is inactive. Removal of kinesin might provide additional binding sites for dynein, cooperatively enhancing transport velocity. Whether the cooperativity of multiple motors can regulate force and velocity has recently been addressed in vivo and in vitro (Kural *et al.*, 2005; Mallik *et al.*, 2005; Levi *et al.*, 2006). Although our experimental data cannot distinguish between these possible mechanisms, they do help to establish that kinesin I is present on the GFP-Exu and GFP-Staufen RNPs and can influence their transport. The regulation of opposing motors on RNPs may provide local control over the directional bias of mRNA transport in different domains within the egg chamber and embryo (Kashina *et al.*, 2004; Ling *et al.*, 2004; Bullock *et al.*, 2006).

Mitochondrial distribution in *Drosophila* oocytes seems to depend on an antagonism between kinesin and dynein motors. Mutations in the kinesin heavy chain enhance the accumulation of mitochondria, whereas mutations in dynein reduce the number of mitochondria that enter the oocyte (Cox and Spradling, 2006). The counterbalance of motor activities on mitochondrial distribution may be mediated by the mitochondrial-specific adapter Milton. The kinesin heavy chain binds directly to Milton, but the function of Milton is independent of the kinesin light chain (Stowers *et al.*, 2002; Glater *et al.*, 2006). Because our results show that the ability of kinesin to antagonize dynein is dependent on both the kinesin heavy and light chains, they therefore indicate that Milton is not the adapter for RNP transport. Similar to kinesin heavy chain mutants, the velocity of RNP

transport is elevated in the light chain mutant backgrounds. This is consistent with observations that the distribution of Cup, a germplasm component, is not affected by the loss of Milton function (Cox and Spradling, 2006).

Current models propose that after the anterior determinant, *bcd*, enters the oocyte, it is actively transported along microtubules to the anterior cortex (Berleth *et al.*, 1988; Cha *et al.*, 2001). We have analyzed the motility of GFP-Exu RNPs and labeled *bcd* RNA in vivo to show that dynein is the motor that actively transports *bcd* RNPs within oocytes. Our observations characterize new aspects of the pathway leading to the anterior localization of *bcd* mRNA in the oocyte. First, we document a striking transition in the motility of GFP-Exu particles (as well as GFP-Staufen) as they are transported across the nurse cell boundary and into the oocyte. The rapid dynein-mediated transport of GFP-Exu particles along linear microtubule tracks in nurse cells is completely suppressed once the particles cross into the oocyte. Instead, kinesin-dependent cytoplasmic streaming passively distributes RNP particles throughout the ooplasm at a reduced velocity (Figure 4) (Palacios and St Johnston, 2002; Snee and Macdonald, 2004). Our results show that neither dynein nor dynactin is required for cytoplasmic streaming. In addition, mutations that disrupt dynein function do not affect the early slow phase of cytoplasmic streaming, nor do they alter the time at which fast streaming is initiated. This latter result differs from a recent report in which the inactivation of dynein by injected antibodies resulted in the induction of fast cytoplasmic streaming (Serbus *et al.*, 2005). An explanation of this discrepancy has not been uncovered, but it could lie in the distinction between the genetic and immunological strategies used to inhibit dynein function.

Despite the cytoplasmic continuum through the ring canal, there is an abrupt change in the motility of GFP-Exu particles at the nurse cell/oocyte boundary. This change has also been detected for GFP-Staufen (Palacios and St Johnston, 2002) and GFP-Aubergine (Snee and Macdonald, 2004). One possibility is that dynein activity on the particles is "switched off," or alternatively, released from particles as they pass through the ring canal. Moreover, the release of kinesin upon entry into the oocyte might trigger the initial induction of cytoplasmic streaming at the anterior. Perhaps a regulatory molecule or complex resides at the ring canal or associates with the network of microtubules at the anterior boundary of the oocyte. Potentially, the dense microtubule network itself could act as a physical barrier to active transport of RNP particles, although this seems unlikely given that particles readily enter the oocyte.

If active transport of GFP-Exu particles entering the oocyte is suppressed, then how does the observed microtubule-dependent, anterior accumulation of GFP-Exu and *bcd* mRNA occur? As previously shown, fluorescently labeled *bcd* mRNA injected into oocytes assembles de novo into RNP particles and accumulates along both the anterior and lateral cortices (Cha *et al.*, 2001). In addition, RNPs assembled in nurse cells and transferred to the oocyte may preferentially accumulate at the anterior cortex. We have directly visualized the rapid, nonpolar transport of de novo *bcd* RNPs along microtubules, and we now show that disruption of dynein activity, but not kinesin, inhibits *bcd* mRNA transport. Thus, the proposed kinesin-mediated recycling of dynein is apparently not required for the anterior transport of the *bcd* determinant (Brendza *et al.*, 2002; Duncan and Warrior, 2002; Januschke *et al.*, 2002). Moreover, in oocytes, the loss of kinesin activity did not elevate the velocity of *bcd* RNP transport. This suggests that kinesin is either not present on *bcd* RNPs assembled in oocytes, or alternatively that kinesin

activity on RNPs is distinctly regulated in oocytes compared with nurse cells. The distinct regulation of kinesin-based transport can be subunit dependent (Palacios and St Johnston, 2002; Ling *et al.*, 2004; this study). In nurse cells, we find the rate of RNP particle transport is accelerated when either Klc or Khc function is removed. Yet, within the oocyte, cytoplasmic streaming is completely arrested in the absence of Khc, but it is retained in the Klc null mutant clones (Palacios and St. Johnston, 2002; this study).

Our results also clearly show that the linear paths taken by newly assembled *bcd* RNPs do not run directly to the cortex, but they are variably oriented relative to the anterior–posterior axis of the oocyte (Supplemental Movie S9). These indirect paths are consistent with the network of randomly oriented microtubules present in the cortical region, and they may account for the relatively slow rate of mRNA accumulation (5–10 min) at the cortex (Figure 6A; also see Cha *et al.*, 2001). Enrichment at the anterior would result from biased transport of particles toward the region of higher microtubule density. Recent studies suggest that maintenance of *bcd* at the anterior of late stage oocytes requires a specialized subset of microtubules nucleated from the anterior cortex as well as dynein function (Weil *et al.*, 2006). Cha *et al.* (2001) have proposed that specific nurse cell factors play a role in the transport of *bcd* along selected microtubules that originate from the anterior cortex (Cha *et al.*, 2001). Similarly, in the case of the dorsal/ventral determinant, *gurken*, MacDougall *et al.* (2003) have suggested accessory factors are required to specify the microtubule subsets along which dynein-mediated transport occurs (MacDougall *et al.*, 2003). Our comparison of the motility of *bcd* RNPs preassembled in the nurse cell cytoplasm versus RNPs assembled on RNA injected directly into the oocyte suggests that in both cases transport is mediated by cytoplasmic dynein. Nonetheless, it will be important to determine whether and how nurse cell factors mediate the preferential recognition of specific microtubules that leads to the restricted anterior localization of the *bcd* determinant.

Based on our observations, we speculate that RNP granules entering the oocyte are no longer rapidly transported but that they disassemble and/or are remodeled into smaller RNPs for delivery to their final destinations. A remodeling step provides an opportunity to modulate the transport, localization, and translational requirements for the associated RNAs (e.g., the posterior determinant, *oskar* mRNA, and the anterior determinant *bcd* mRNA). Our observation that the late posterior localization of GFP-Exu depends on its early anterior localization is consistent with the possible remodeling of RNPs. As suggested by Bullock *et al.* (2006) changes in RNP motor composition may only occur during the assembly steps (Bullock *et al.*, 2006). Remodeling of RNPs may affect other steps in the mRNA localization pathway as well. For example, in *Saccharomyces cerevisiae*, Gonsalvez *et al.* (2004) have shown that the anchoring of *ASH1* mRNA at the tip of budding cells requires the remodeling of the Myo4p–She3p–She2p transport complex (Gonsalvez *et al.*, 2004). More work is required to test this hypothesis and to investigate the change in RNP composition and associated motor activities.

REFERENCES

Berleth, T., Burri, M., Thoma, G., Bopp, D., Richstein, S., Frigerio, G., Noll, M., and Nusslein-Volhard, C. (1988). The role of localization of bicoid RNA in organizing the anterior pattern of the *Drosophila* embryo. EMBO J. *7*, 1749–1756.

Boylan, K. L., and Hays, T. S. (2002). The gene for the intermediate chain subunit of cytoplasmic dynein is essential in *Drosophila*. Genetics *162*, 1211–1220.

Boylan, K., Serr, M., and Hays, T. (2000). A molecular genetic analysis of the interaction between the cytoplasmic dynein intermediate chain and the glued (dynactin) complex. Mol. Biol. Cell *11*, 3791–3803.

Brand, A. H., and Perrimon, N. (1993). Targeted gene expression as a means of altering cell fates and generating dominant phenotypes. Development *118*, 401–415.

Brendza, R. P., Serbus, L. R., Duffy, J. B., and Saxton, W. M. (2000). A function for kinesin I in the posterior transport of oskar mRNA and Staufen protein. Science *289*, 2120–2122.

Brendza, R. P., Serbus, L. R., Saxton, W. M., and Duffy, J. B. (2002). Posterior localization of dynein and dorsal-ventral axis formation depend on kinesin in *Drosophila* oocytes. Curr. Biol. *12*, 1541–1545.

Bullock, S. L., Nicol, A., Gross, S. P., and Zicha, D. (2006). Guidance of bidirectional motor complexes by mRNA cargoes through control of dynein number and activity. Curr. Biol. *16*, 1447–1452.

Cha, B. J., Koppetsch, B. S., and Theurkauf, W. E. (2001). In vivo analysis of *Drosophila* bicoid mRNA localization reveals a novel microtubule-dependent axis specification pathway. Cell *106*, 35–46.

Chou, T. B., Noll, E., and Perrimon, N. (1993). Autosomal P[ovoD1] dominant female-sterile insertions in *Drosophila* and their use in generating germ-line chimeras. Development *119*, 1359–1369.

Chou, T. B., and Perrimon, N. (1996). The autosomal FLP-DFS technique for generating germline mosaics in *Drosophila melanogaster*. Genetics *144*, 1673–1679.

Cox, R. T., and Spradling, A. C. (2006). Milton controls the early acquisition of mitochondria by *Drosophila* oocytes. Development *133*, 3371–3377.

Duncan, J. E., and Warrior, R. (2002). The cytoplasmic dynein and kinesin motors have interdependent roles in patterning the *Drosophila* oocyte. Curr. Biol. *12*, 1982–1991.

Echeverri, C. J., Paschal, B. M., Vaughan, K. T., and Vallee, R. B. (1996). Molecular characterization of the 50-kD subunit of dynactin reveals function for the complex in chromosome alignment and spindle organization during mitosis. J. Cell Biol. *132*, 617–633.

Emmons, S., Phan, H., Calley, J., Chen, W., James, B., and Manseau, L. (1995). Cappuccino, a *Drosophila* maternal effect gene required for polarity of the egg and embryo, is related to the vertebrate limb deformity locus. Genes Dev. *9*, 2482–2494.

Fan, S. S., and Ready, D. F. (1997). Glued participates in distinct microtubule-based activities in *Drosophila* eye development. Development *124*, 1497–1507.

Forrest, K. M., and Gavis, E. R. (2003). Live imaging of endogenous RNA reveals a diffusion and entrapment mechanism for nanos mRNA localization in *Drosophila*. Curr. Biol. *13*, 1159–1168.

Gepner, J., Li, M., Ludmann, S., Kortas, C., Boylan, K., Iyadurai, S. J., McGrail, M., and Hays, T. S. (1996). Cytoplasmic dynein function is essential in *Drosophila melanogaster*. Genetics *142*, 865–878.

Glater, E. E., Megeath, L. J., Stowers, R. S., and Schwarz, T. L. (2006). Axonal transport of mitochondria requires milton to recruit kinesin heavy chain and is light chain independent. J. Cell Biol. *173*, 545–557.

Glotzer, J. B., Saffrich, R., Glotzer, M., and Ephrussi, A. (1997). Cytoplasmic flows localize injected oskar RNA in *Drosophila* oocytes. Curr. Biol. *7*, 326–337.

Gonsalvez, G. B., Little, J. L., and Long, R. M. (2004). ASH1 mRNA anchoring requires reorganization of the Myo4p-She3p-She2p transport complex. J. Biol. Chem. *279*, 46286–46294.

Granadino, B., San Juan, A., Santamaria, P., and Sanchez, L. (1992). Evidence of a dual function in fl(2)d, a gene needed for Sex-lethal expression in *Drosophila melanogaster*. Genetics *130*, 597–612.

Januschke, J., Gervais, L., Dass, S., Kaltschmidt, J. A., Lopez-Schier, H., St Johnston, D., Brand, A. H., Roth, S., and Guichet, A. (2002). Polar transport in the *Drosophila* oocyte requires Dynein and Kinesin I cooperation. Curr. Biol. *12*, 1971–1981.

Karess, R. E., and Rubin, G. M. (1984). Analysis of P transposable element functions in *Drosophila*. Cell *38*, 135–146.

Kashina, A. S., Semenova, I. V., Ivanov, P. A., Potekhina, E. S., Zaliapin, I., and Rodionov, V. I. (2004). Protein kinase A, which regulates intracellular transport, forms complexes with molecular motors on organelles. Curr. Biol. *14*, 1877–1881.

Kloc, M., and Etkin, L. D. (2005). RNA localization mechanisms in oocytes. J. Cell Sci. *118*, 269–282.

Koch, E. A., and Spitzer, R. H. (1983). Multiple effects of colchicine on oogenesis in *Drosophila*: induced sterility and switch of potential oocyte to nurse-cell developmental pathway. Cell Tissue Res. *228*, 21–32.

Kural, C., Kim, H., Syed, S., Goshima, G., Gelfand, V. I., and Selvin, P. R. (2005). Kinesin and dynein move a peroxisome in vivo: a tug-of-war or coordinated movement? Science *308*, 1469–1472.

Levi, V., Serpinskaya, A. S., Gratton, E., and Gelfand, V. (2006). Organelle transport along microtubules in *Xenopus* melanophores: evidence for cooperation between multiple motors. Biophys. J. *90*, 318–327.

Lin, M. D., Fan, S. J., Hsu, W. S., and Chou, T. B. (2006). *Drosophila* decapping protein 1, dDcp1, is a component of the oskar mRNP complex and directs its posterior localization in the oocyte. Dev. Cell *10*, 601–613.

Ling, S. C., Fahrner, P. S., Greenough, W. T., and Gelfand, V. I. (2004). Transport of *Drosophila* fragile X mental retardation protein-containing ribonucleoprotein granules by kinesin-1 and cytoplasmic dynein. Proc. Natl. Acad. Sci. USA *101*, 17428–17433.

Lipshitz, H. D., and Smibert, C. A. (2000). Mechanisms of RNA localization and translational regulation. Curr. Opin. Genet. Dev. *10*, 476–488.

MacDougall, N., Clark, A., MacDougall, E., and Davis, I. (2003). *Drosophila* gurken (TGFalpha) mRNA localizes as particles that move within the oocyte in two dynein-dependent steps. Dev. Cell *4*, 307–319.

Mallik, R., Petrov, D., Lex, S. A., King, S. J., and Gross, S. P. (2005). Building complexity: an in vitro study of cytoplasmic dynein with in vivo implications. Curr. Biol. *15*, 2075–2085.

Martin, M., Iyadurai, S. J., Gassman, A., Gindhart, J. G., Jr., Hays, T. S., and Saxton, W. M. (1999). Cytoplasmic dynein, the dynactin complex, and kinesin are interdependent and essential for fast axonal transport. Mol. Biol. Cell *10*, 3717–3728.

McGrail, M., Gepner, J., Silvanovich, A., Ludmann, S., Serr, M., and Hays, T. S. (1995). Regulation of cytoplasmic dynein function in vivo by the *Drosophila* Glued complex. J. Cell Biol. *131*, 411–425.

McGrail, M., and Hays, T. S. (1997). The microtubule motor cytoplasmic dynein is required for spindle orientation during germline cell divisions and oocyte differentiation in *Drosophila*. Development *124*, 2409–2419.

Meng, J., and Stephenson, E. C. (2002). Oocyte and embryonic cytoskeletal defects caused by mutations in the *Drosophila* swallow gene. Dev. Genes Evol. *212*, 239–247.

Navarro, C., Puthalakath, H., Adams, J. M., Strasser, A., and Lehmann, R. (2004). Egalitarian binds dynein light chain to establish oocyte polarity and maintain oocyte fate. Nat. Cell Biol. *6*, 427–435.

Palacios, I. M., and St Johnston, D. (2002). Kinesin light chain-independent function of the Kinesin heavy chain in cytoplasmic streaming and posterior localisation in the *Drosophila* oocyte. Development *129*, 5473–5485.

Pokrywka, N. J., and Stephenson, E. C. (1991). Microtubules mediate the localization of bicoid RNA during *Drosophila* oogenesis. Development *113*, 55–66.

Rorth, P. (1998). Gal4 in the *Drosophila* female germline. Mech. Dev. *78*, 113–118.

Rosales-Nieves, A. E., Johndrow, J. E., Keller, L. C., Magie, C. R., Pinto-Santini, D. M., and Parkhurst, S. M. (2006). Coordination of microtubule and microfilament dynamics by *Drosophila* Rho1, Spire and Cappuccino. Nat. Cell Biol. *8*, 367–376.

Schroer, T. A., Schnapp, B. J., Reese, T. S., and Sheetz, M. P. (1988). The role of kinesin and other soluble factors in organelle movement along microtubules. J. Cell Biol. *107*, 1785–1792.

Serbus, L. R., Cha, B. J., Theurkauf, W. E., and Saxton, W. M. (2005). Dynein and the actin cytoskeleton control kinesin-driven cytoplasmic streaming in *Drosophila* oocytes. Development *132*, 3743–3752.

Shav-Tal, Y., and Singer, R. H. (2005). RNA localization. J. Cell Sci. *118*, 4077–4081.

Snee, M. J., and Macdonald, P. M. (2004). Live imaging of nuage and polar granules: evidence against a precursor-product relationship and a novel role for Oskar in stabilization of polar granule components. J. Cell Sci. *117*, 2109–2120.

St Johnston, D. (2005). Moving messages: the intracellular localization of mRNAs. Nat. Rev. Mol. Cell Biol. *6*, 363–375.

Steinhauer, J., and Kalderon, D. (2006). Microtubule polarity and axis formation in the *Drosophila* oocyte. Dev. Dyn. *235*, 1455–1468.

Stowers, R. S., Megeath, L. J., Gorska-Andrzejak, J., Meinertzhagen, I. A., and Schwarz, T. L. (2002). Axonal transport of mitochondria to synapses depends on milton, a novel *Drosophila* protein. Neuron *36*, 1063–1077.

Swaroop, A., Swaroop, M., and Garen, A. (1987). Sequence analysis of the complete cDNA and encoded polypeptide for the Glued gene of *Drosophila melanogaster*. Proc. Natl. Acad. Sci. USA *84*, 6501–6505.

Theurkauf, W. E. (1994). Premature microtubule-dependent cytoplasmic streaming in cappuccino and spire mutant oocytes. Science *265*, 2093–2096.

Theurkauf, W. E., Alberts, B. M., Jan, Y. N., and Jongens, T. A. (1993). A central role for microtubules in the differentiation of *Drosophila* oocytes. Development *118*, 1169–1180.

Theurkauf, W. E., and Hazelrigg, T. I. (1998). In vivo analyses of cytoplasmic transport and cytoskeletal organization during *Drosophila* oogenesis: characterization of a multi-step anterior localization pathway. Development *125*, 3655–3666.

Valetti, C., Wetzel, D. M., Schrader, M., Hasbani, M. J., Gill, S. R., Kreis, T. E., and Schroer, T. A. (1999). Role of dynactin in endocytic traffic: effects of dynamitin overexpression and colocalization with CLIP-170. Mol. Biol. Cell *10*, 4107–4120.

Wang, S., and Hazelrigg, T. (1994). Implications for bcd mRNA localization from spatial distribution of exu protein in *Drosophila* oogenesis. Nature *369*, 400–403.

Waterman-Storer, C. M., and Holzbaur, E. L. (1996). The product of the *Drosophila* gene, Glued, is the functional homologue of the p150Glued component of the vertebrate dynactin complex. J. Biol. Chem. *271*, 1153–1159.

Waterman-Storer, C. M., Karki, S. B., Kuznetsov, S. A., Tabb, J. S., Weiss, D. G., Langford, G. M., and Holzbaur, E. L. (1997). The interaction between cytoplasmic dynein and dynactin is required for fast axonal transport. Proc. Natl. Acad. Sci. USA *94*, 12180–12185.

Weil, T. T., Forrest, K. M., and Gavis, E. R. (2006). Localization of bicoid mRNA in late oocytes is maintained by continual active transport. Dev. Cell *11*, 251–262.

Wilhelm, J. E., Mansfield, J., Hom-Booher, N., Wang, S., Turck, C. W., Hazelrigg, T., and Vale, R. D. (2000). Isolation of a ribonucleoprotein complex involved in mRNA localization in *Drosophila* oocytes. J. Cell Biol. *148*, 427–440.